CDF/ANAL/JET/CDFR/6280
Version 2.0
January 24,2003
Rev. June 6, 2003

Generic Jet Energy Corrections for Run II data used for the Winter Conferences

J-F Arguin, A. A. Bhatti, C. A. Currat, R. Erbacher,
L. Galtieri, R. Harris, B. Heinemann, H. S. Kim, G. Latino, J. Lys,
R. Madrak, M. Martinez, W. Sakumoto, M. Shochet, M. Schmitt

Jet Corrections Group

Abstract

The generic jet energy corrections to be applied to Run II data presented at the Winter Conferences are described. The η dependent corrections are determined by the di-jet balancing technique, i.e., by normalizing the measured jet P_T in a given η bin to the central calorimeter ($0.2 < |\eta| < 0.6$). In the central region the CEM energy scale is set by the Z^0 mass peak, the CHA energy scale is set equal to the Run I scale, by using high P_T and J/Ψ muons. The starting strategy has been to establish that the raw jet energy scale of the central calorimeter is the same as for Run I, and then use the same absolute corrections as those used in Run I. The photon-jet data sets are used to compare the raw jet energy scale to the Run I scale. A discrepancy of $\sim$ 5% is observed in the raw jet energy scale. We correct the jets by this factor. We find that data and Monte Carlo simulation do not agree, so we provide separate relative corrections for data and Monte Carlo. All the corrections are installed in offline V4.9.1 and are to be applied to data processed with offline version V4.9.1.

1 Introduction

The raw jet energies measured in the calorimeter must be corrected for detector effects before they can be compared to physics predictions/models.

The generic jet energy corrections consist of many steps [1], so that, depending on the physics analysis, a subset of these corrections can be applied. A heavy quark jet containing one or more neutrinos will need extra corrections which are not included here. Generic jet corrections include:

- Relative jet energy corrections to make the calorimeter response uniform in η (determined from data).
- Multiple interactions corrections (determined from data).
- Absolute jet energy corrections to convert calorimeter cluster P_T to the $\sum(P_T)$ of the particles in the cone (uses calorimeter calibration and jet fragmentation properties, as well as simulation tuned to test beam and $p\bar{p}$ data).
- Underlying event subtraction to obtain particle level "jet" P_T (determined from data).
- Out-of-cone corrections to get to the full "parent parton" P_T.

In Run I all of these corrections were included in JTC96X. See CDF-1513 [1] for details of the methods used. Details of the final corrections used in JTC96X and the systematic uncertainties assigned to each correction can be found in Ref. [2] (and references therein).

It should be noted here that the absolute and out-of-cone corrections derived in Run I were obtained for generic QCD jets generated with the $2 \rightarrow 2$ QCD process. The underlying event was assumed to be the one found in minbias events. These corrections are process dependent and one should use them with caution. Also, a flat spectrum is assumed so that the user can add the information of the jet P_T spectrum for the process being studied.

The geometry of the Run II detector is different than that of Run I. The old gas calorimeters have been replaced by a new plug calorimeter based on scintillator tiles, read out by wavelength shifting fibers that transport the signals to phototubes. Fig. 1 shows the calorimeters configuration in Run II.

2 Relative Jet Energy Corrections

The first step in jet energy corrections is to correct the jets for any variation in response with detector η. The transverse energy of the two jets in a $2 \rightarrow 2$ process should be equal. This property is used to scale jets outside the $0.2 < |\eta| < 0.6$ region to jets inside this region. The central calorimeters CEM/CHA are the best

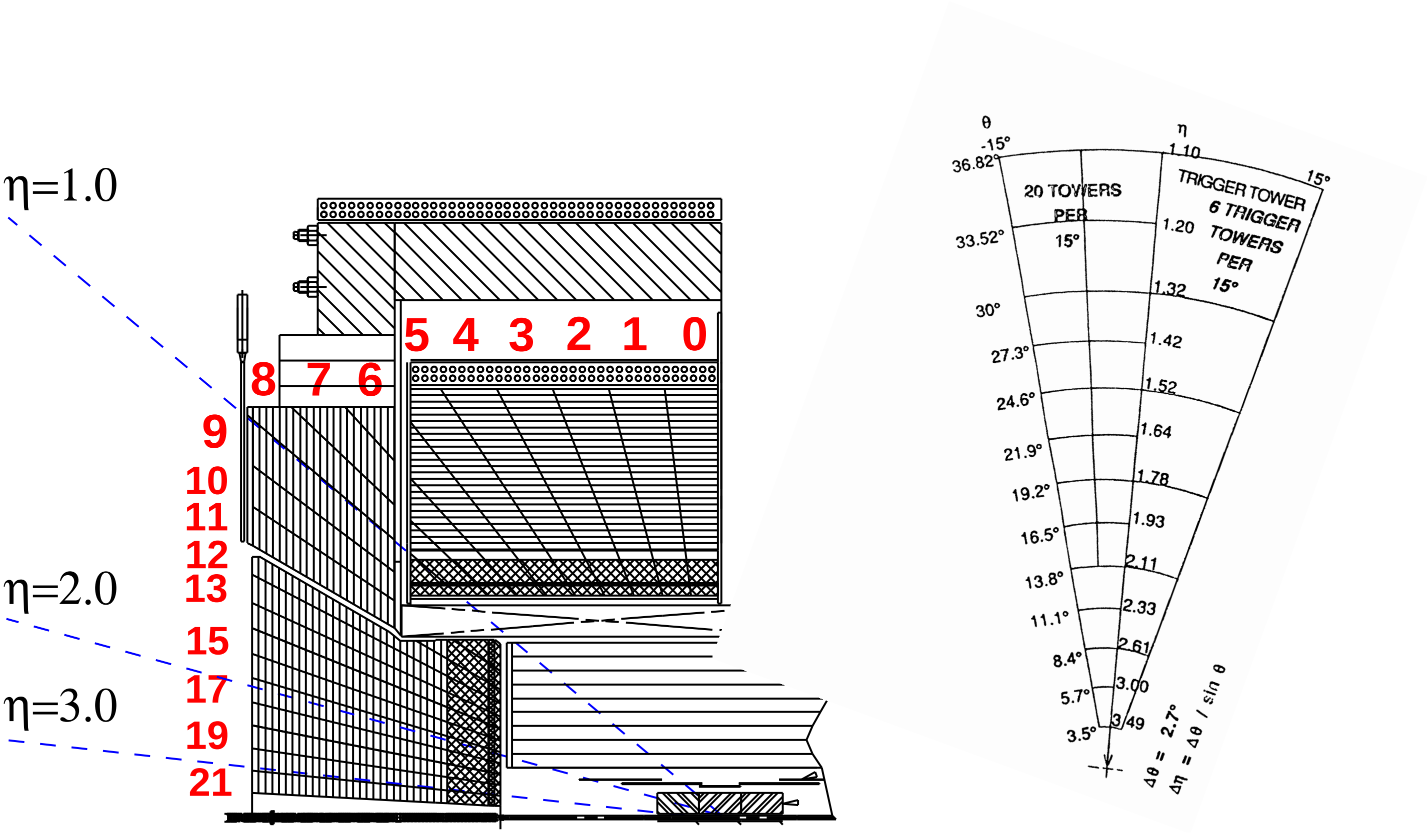

Figure 1: The run II CDF detector calorimeters. Left: one quater section. The central (CEM, CHA) and WHA calorimeters have notchanged, whereas the plug calorimeters (PEM, PHA) are new. The numbers refer to the nomenclature for the towers. Right: the plug wedge configuration. Both the angle to the beam axis and the η values are given.

understood calorimeters in CDF and the selected region is far away from the cracks. Before proceeding with relative corrections we have to verify that the energy scale of the central calorimeters (CEM and CHA) is stable and the energy calibration is the same as in Run I. This is discussed in Sec. 3.

The Jet_20, Jet_50, Jet_70 and Jet_100 data are used (processed with offline V4.9.1). We define as "trigger jet" a jet within the $0.2 < |\eta| < 0.6$ region and call the other jet "probe jet". If two jets lie in the "trigger jet" region, we choose one of them at random.

The correction factor to make, *on average*, the P_T^{Probe} scale equal to P_T^{Trig} is given by:

$$P_T^{Probe}/P_T^{Trigger} = 1 + 2\bar{B}/(2 - \bar{B})$$

where $\bar{B}$ is

$$\bar{B} = 2(P_T^{Probe} - P_T^{Trig})/(P_T^{Probe} + P_T^{Trig})$$

averaged over the whole data set.

In Run I (CDF-1513), the Missing E_T Projection Fraction (MPF) along the probe jet was used. It is defined as

$$MPF = \quad 2\overrightarrow{MET} \cdot \hat{P}_T^{Probe}/(P_T^{Probe} + P_T^{Trig})$$

where

$$\overrightarrow{MET} \cdot \hat{P}_T^{Probe} = P_T^{Probe} - P_T^{Trig}$$

The average correction factor is then:

$$P_T^{Trigger}/P_T^{Probe} = 1 + 2M\bar{P}F/(2 - M\bar{P}F)$$

This method is claimed to be "less dependent on how well the third jet is clustered and results in a better jet balancing resolution" (see CDF-835).

However, the MPF method is not used here because the missing E_T in Run II was not well understood when these studies were started.

For the results presented in this note, the di-jet balancing was done using the event selection cuts described in Table 1.

The $P_T^{Ave,min}$ cut minimizes any trigger bias and $P_T^{(3),max}$ selects relatively clean "di-jet" events where two leading jets are expected to balance. $P_T^{Ave,min}$ and $P_T^{(3),max}$ depend on the data set and are given in Table 2. The effect of variation of $P_T^{Ave,min}$ on the Jet_20 sample is shown in Fig. 2.

Table 1: Cuts used to determine relative jet energy corrections.

Missing E_T significance	$\overrightarrow{MET}/\sqrt{\sum E_T}$	$\leq$	3.0
z-vertex	$\lvert z_{vertex}\rvert$	$\leq$	60 cm
Average P_T of two leading jets	$(P_T^1 + P_T^2)/2$	$\geq$	$P_T^{Ave,min}$ GeV
Opening angle between two leading jets	$\Delta\phi$	$\geq$	2.5 radians
P_T of third Jet	P_T^3	$\leq$	$P_T^{(3),max}$ GeV

Table 2: Cuts (in GeV/c) used for different data sets.

	$P_T^{Ave,min}$	$P_T^{(3),max}$
Jet_20	25	8
Jet_50	55	8
Jet_70	75	10
Jet_100	105	10

2.1 Time Dependence of the Plug Calorimeters Gains

We use only the PEM energy for the electromagnetic energy in the plug calorimeter. Studies on including the PPR energy are still in progress [3].

In August 2002 laser and plug data showed that the response of the plug calorimeters is changing with time, mostly due to aging of the phototubes. Since then a procedure has been setup to correct the data for this time variation [4]. For the time being the data have been divided in three run periods and the corrections determined separately for each period. See Table 3.

Table 3: Data sets used for the three run periods.

Set	dates	Run interval
1	Feb 4/02-Jun 2/02	138425-145654
2	Jun 19/02-Sep 24/02	146841-152400
3	Oct 4/02-Jan 12/03	152490-156458

The correction factors are shown in Figs. 3 to 10. Figs. 11 to 13 show the spline interpolation for different cone sizes for the four data sets. Fig. 14 shows the residual corrections for some of the samples. From these plots we derive the uncertainty on the corrections to be $\pm$ 2%.

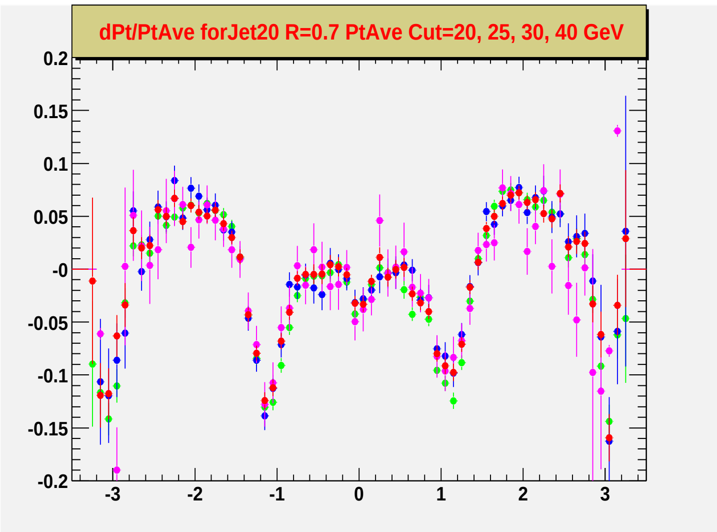

Figure 2: Fractional difference, $\bar{B}$, between P_T of "trigger" and "probe" jets for $(P_T^{(1)} + P_T^{(2)})/2 \geq 20$, 25, 30 and 40 GeV for the Jet_20 data set. There is no significant dependence of B on this cut. For the present analysis we use the data with $P_T^{Ave} \geq 25$ GeV.

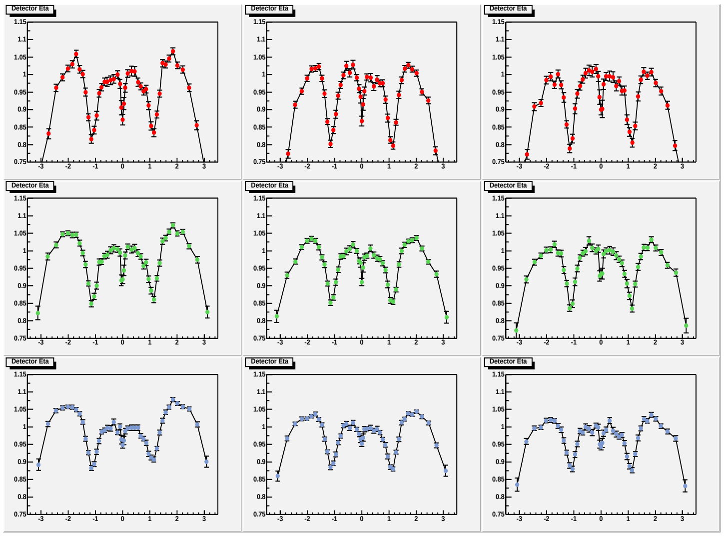

Figure 3: Correction factors before relative corrections for Jet_20 data, cone radii R=0.4 (top), 0.7 (middle) and 1.0 (bottom), for three different running periods: Feb. 4-June 2, 2002 (left), June 19-Sept. 24, 2002 (middle) and Oct. 4-Jan. 12, 2003 (right).

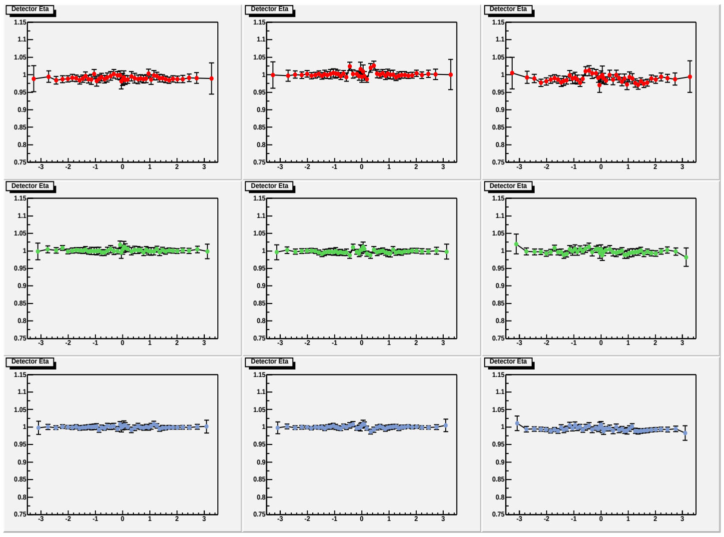

Figure 4: Correction factors after relative corrections for Jet_20 data, radii R=0.4 (top), 0.7 (middle) and 1.0 (bottom), for three different running periods: Feb. 4-June 2, 2002 (left), June 19-Sept. 24, 2002 (middle) and Oct. 4-Jan. 12, 2003 (right).

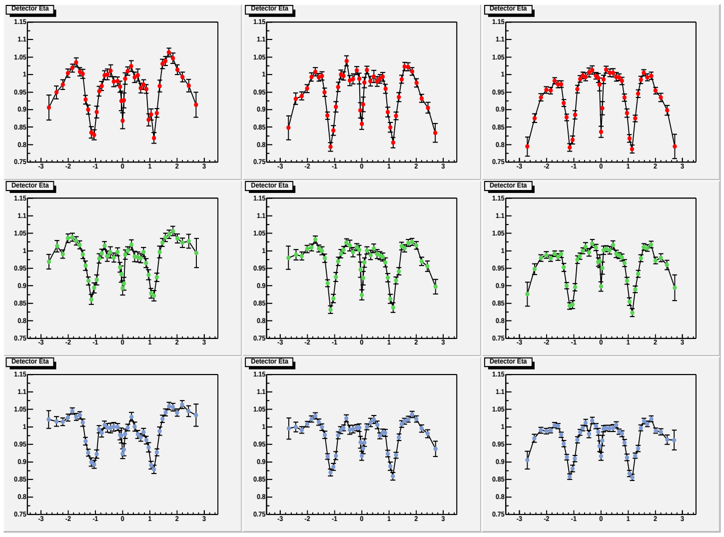

Figure 5: Correction factors before the relative corrections for Jet_50 data, radii R=0.4 (top), 0.7 (middle) and 1.0 (bottom), for three different running periods: Feb. 4-June 2, 2002 (left), June 19-Sept. 24, 2002 (middle) and Oct. 4-Jan. 12, 2003 (right).

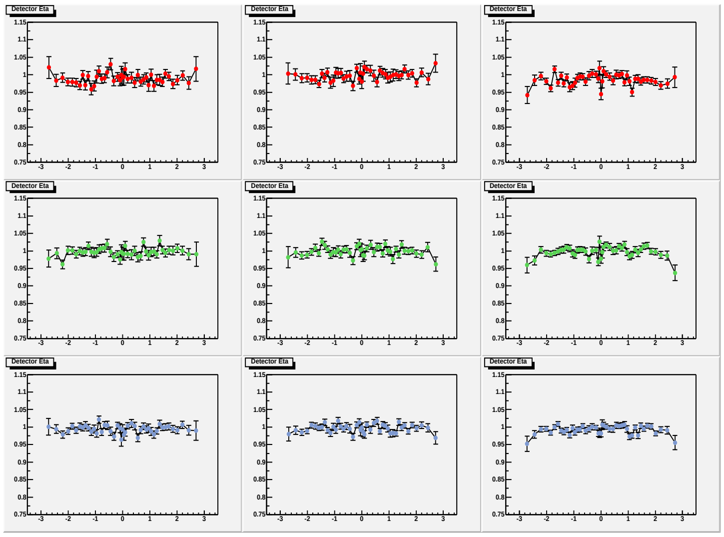

Figure 6: Correction factors after the relative corrections for Jet_50 data, radii R=0.4 (top), 0.7 (middle) and 1.0 (bottom), for three different running periods: Feb. 4-June 2, 2002 (left), June 19-Sept. 24, 2002 (middle) and Oct. 4-Jan. 12, 2003 (right).

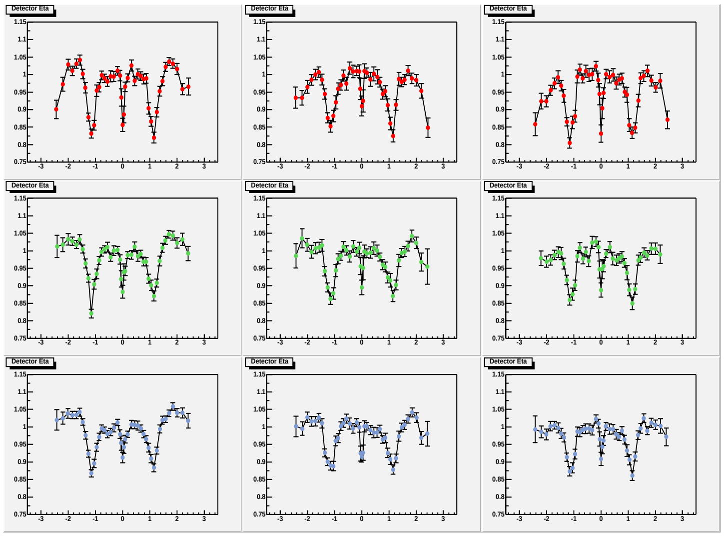

Figure 7: Correction factors before the relative corrections for Jet_70 data, radii R=0.4 (top), 0.7 (middle) and 1.0 (bottom), for three different running periods: Feb. 4-June 2, 2002 (left), June 19-Sept. 24, 2002 (middle) and Oct. 4-Jan. 12, 2003 (right).

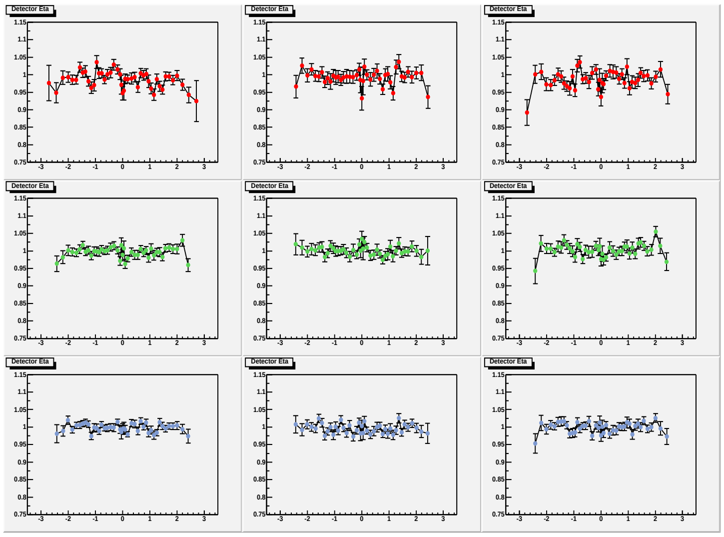

Figure 8: Correction factors after relative corrections for Jet_70 data, radii R=0.4 (top), 0.7 (middle) and 1.0 (bottom), for three different running periods: Feb. 4-June 2, 2002 (left), June 19-Sept. 24, 2002 (middle) and Oct. 4-Jan. 12, 2003 (right).

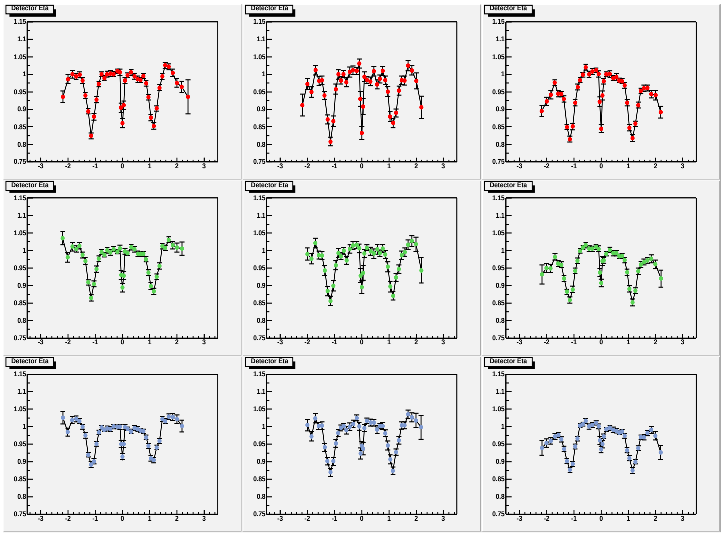

Figure 9: Correction factors before the relative corrections for Jet_100 data, radii R=0.4 (top), 0.7 (middle) and 1.0 (bottom), for three different running periods: Feb. 4-June 2, 2002 (left), June 19-Sept. 24, 2002 (middle) and Oct. 4-Jan. 12, 2003 (right).

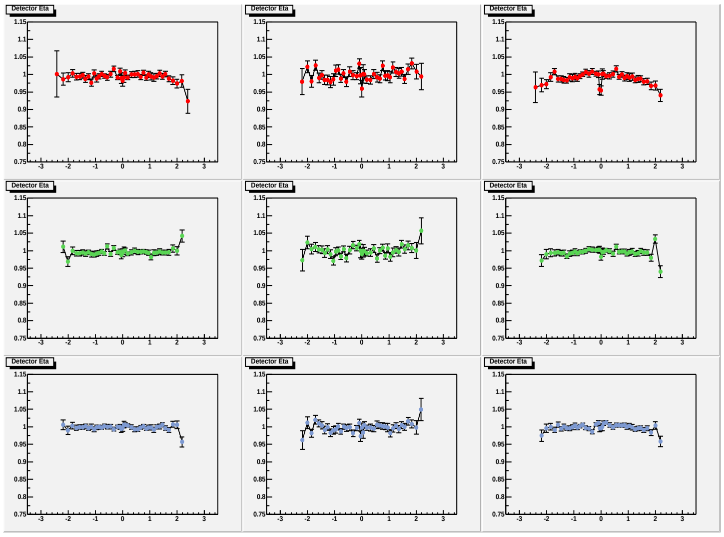

Figure 10: Correction factor after relative corrections for Jet_100 data, radii R=0.4 (top), 0.7 (middle) and 1.0 (bottom), for three different running periods: Feb. 4-June 2, 2002 (left), June 19-Sept. 24, 2002 (middle) and Oct. 4-Jan. 12, 2003 (right).

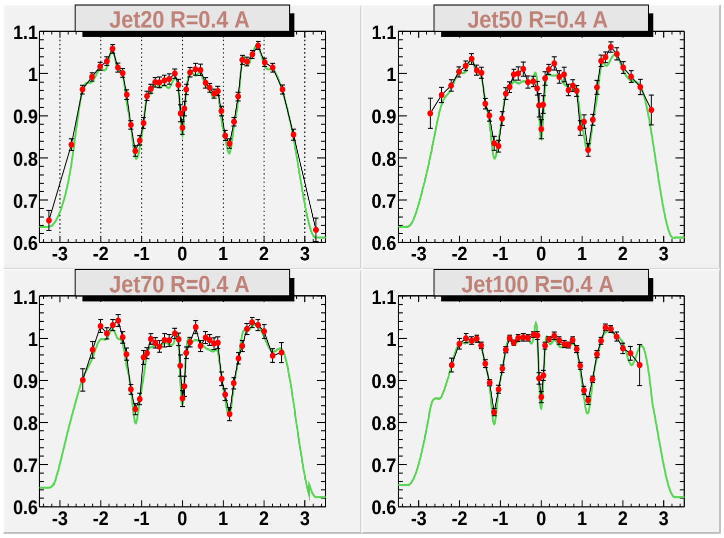

Figure 11: Spline-interpolation correction factors for Jet_20, Jet_50, Jet_70 and Jet_100 data for cone size R=0.4. Actual corrections and spline-interpolation agree to better than 1-2%. The wiggles outside the data region are ugly but not important.

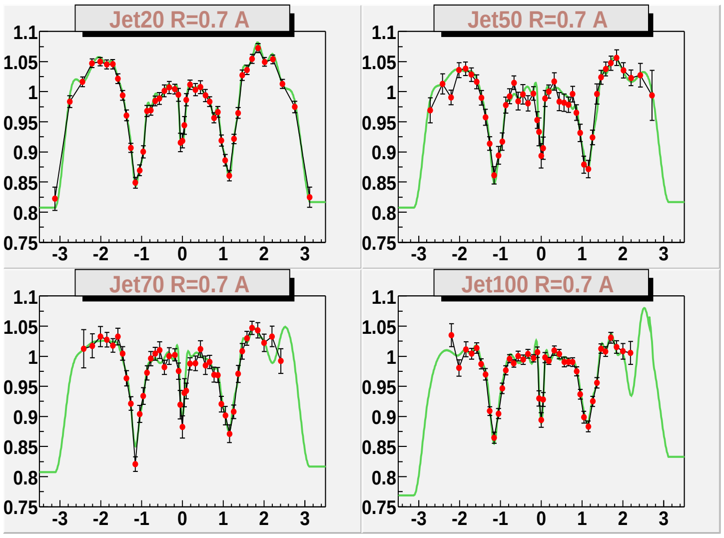

Figure 12: Spline-interpolation of Jet_20, Jet_50, Jet_70 and Jet_100 data for cone size R=0.7. The wiggles outside the data region are ugly but not important.

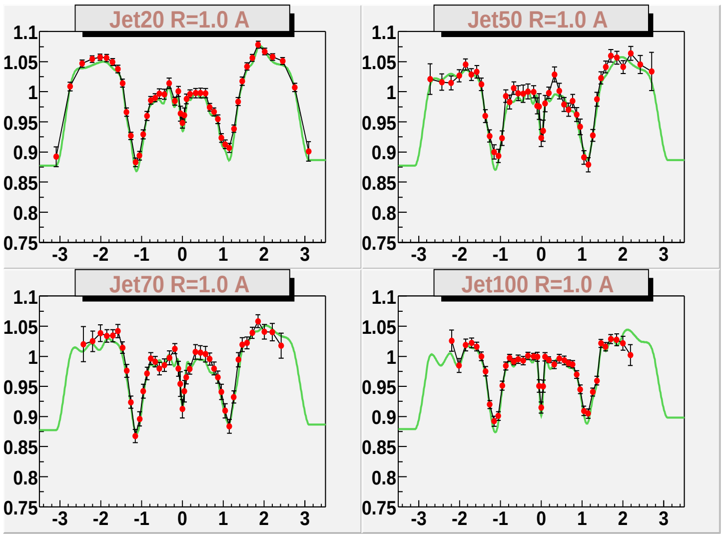

Figure 13: Spline-interpolation of Jet_20, Jet_50, Jet_70 and Jet_100 data for cone size R=1.0.

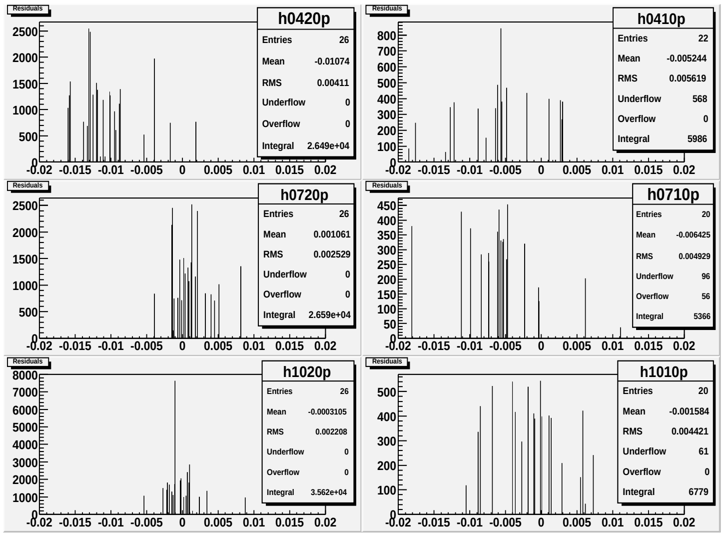

Figure 14: Residual correction factors after application of the relative corrections for Jet_20 (left) and Jet_100 data (right) for R=0.4 (top), 0.7 (middle) and 1.0 (bottom) for data taken between Feb.4-June 2, 2002. We estimate the systematic uncertainty on the relative corrections to be $\pm 2\%$ which is the width of the above distributions.

The relative corrections averaged over the runs in each run period are shown in Fig. 15. Use of run-by-run corrections, when available, will improve the jet energy resolution and reduce the systematic uncertainties on the correction factors.

2.2 Comparison with Run I Relative Jet Energy Corrections

The Run II relative corrections for Jet_20 data are compared with the Run I (JTC96X) corrections in Fig. 16. The JTC96X corrections are evaluated for jets with $P_T = 25$ GeV. The over all agreement is reasonable in the central region. They agree in the $|\eta| = 0$ crack region. There is a smaller dip by $\sim 8\%$ around $|\eta| = 1.1$. This is due in part to the fact that there is less inactive material in the crack region. The plug now starts at 37^0, about $|\eta| = 1.1$, (see Fig. 1). Tower 9 gets more energy in the Run II geometry (previously lost in the gas calorimeter), since the PEM is now beveled off at 37^0. See Fig. 16. The plug-forward 10^0 crack, $|\eta| = 2.4$, has disappeared as expected.

2.3 Relative Corrections for Monte Carlo Data

The CDF calorimeter simulation has been tuned to the single particle response observed in test beam data for particle momenta ≥ 7 GeV in the central calorimeter and 8 GeV in the plug calorimeter [5]. Also $p\bar{p}$ data has been used in the central calorimeters for particle momenta < 4 GeV [6]. Full geometry of the detector has

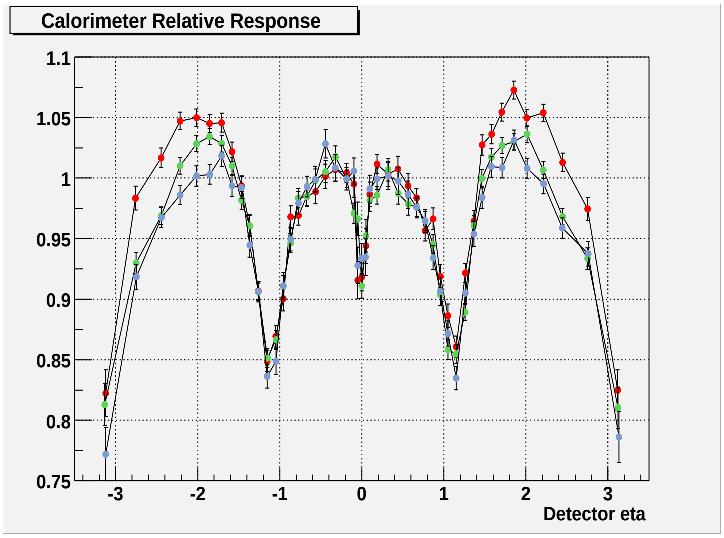

Figure 15: Variation of plug energy scale with time, assuming the central calorimeter scale to be constant. The three run periods are Feb. 4-June 2, 2002 (upper curve); June 19-Sept. 24, 2002 (middle curve); Oct. 4-Jan. 12, 2003 (lower curve). The Jet_20 data was used here and jet cone size of R=0.4.

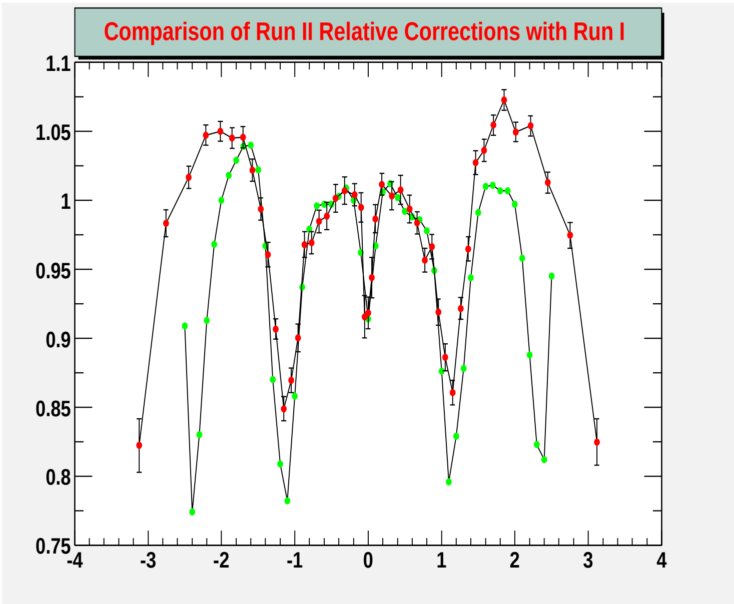

Figure 16: Comparison of Run II relative corrections to those for Run I (JTC96X, lower curve at $|\eta|$=2). These corrections are for Jet_20 data evaluated at 25 GeV data and for jet cone radius R=0.4. They agree in the $|\eta| = 0$ crack region. The difference of $\sim$ 8% around $|\eta| = 1.1$ is due in part to the fact that in Run II there is less inactive material in the crack region. The new plug geometry increases considerably the good η region for jet measurements.

been implemented in simulation. However, despite best efforts, the simulation is not able to reproduce the actual detector response in details especially close to un-instrumented regions, as seen around $|\eta| = 1$.

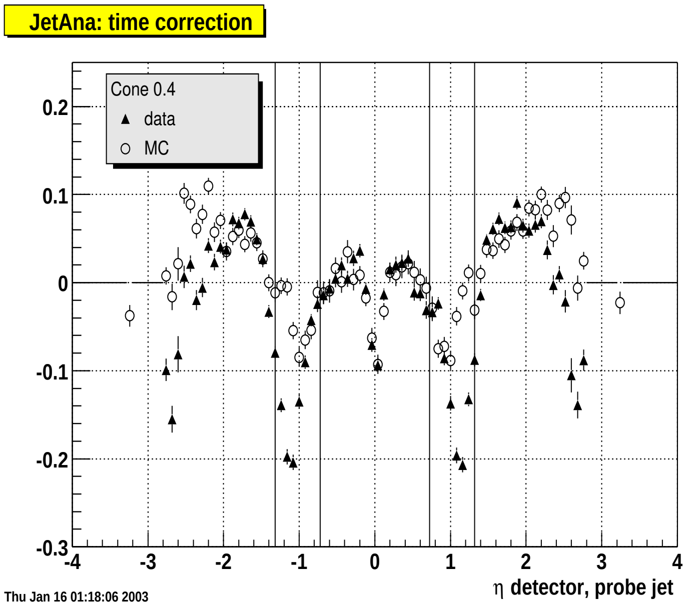

Figure 17: Relative response, $\bar{B}$, of simulated data compared to the Jet_20 data taken in the Feb. 4-Nov., 2002 period. A jet cone size R=0.4 is used. The Jet_20 data has been corrected for time dependent gains observed in the plug calorimeter.

Details on Monte Carlo and data comparison can be found in [7]. At this purpose three million di-jet events were generated with $P_T^{min} > 18$ GeV, using PYTHIA V6.203 with Rick Field "tune A" for the underlying event. The relative jet response, $\bar{B}$, for the simulation has been obtained using the same event selections as for the data, described in Section 2, and applying the di-jet balance technique. In Fig.17 the Monte Carlo is compared with the Jet_20 data for the cone radius of 0.4. The Jet_20 data has been corrected for plug gain degradation using time dependent correction factors determined from laser and source data [4]. These corrections are given as a function of run number and tower number. The corrections used here are approximate because, instead of correcting each tower and reclustering to obtain a new jet, we correct the jet with the factor that applies to the tower the jet points to.

It is easy to see that in the crack region the data and the MC do not agree. It is not clear if the disagreement is due to energy scale problems in the data (WHA in particular) or to problems with the detector simulation. We also note that for $|\eta| > 2$ there is a large disagreement between data and Monte Carlo. This is another area that needs to be investigated.

Because of these disagreements we provide separate relative corrections for the Monte Carlo simulation and the dta at this time. Corrections determined from these

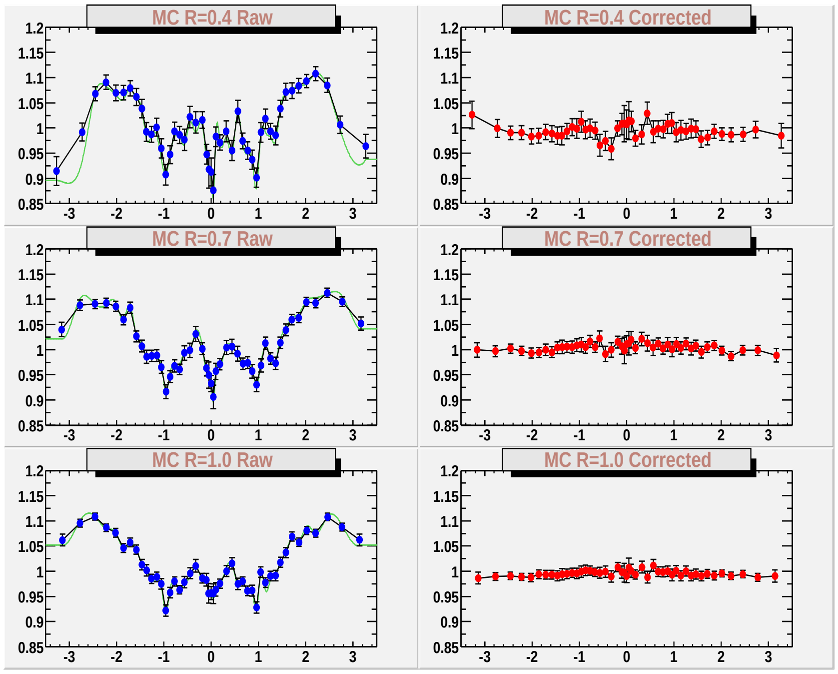

Figure 18: Relative jet corrections for Monte Carlo data for three jet cones (0.4, 0.7, 1.0) (left). Correction factors after the relative corrections have been applied for the three jet cones (right).

Monte Carlo data are shown in Fig.18 for three cone sizes.

2.4 Summary of Current Relative Jet Corrections

- The plug jet energy scale is set to the central scale using di-jet balancing.
- The systematic uncertainty of the energy scale in $|\eta| < 0.1$ and $|\eta| > 0.6$ relative to the central scale is 2%. This is the contribution from uncertainty in procedure/cuts, remaining wiggles and time dependence. For the crack region there are additional contributions as discussed in [8].
- Relative jet energy corrections for Monte Carlo data are determined separately. See Ref [8] for discussion of the systematic uncertainties..

3 Scale Corrections in the Central Calorimeters (going back to Run 0 Raw Jet Energy Scale)

The absolute energy corrections, which take the measured calorimeter energy to the $\sum P_T$ of the particles within a cone, were determined in 1991 [1]. The same corrections, modulo a scale factor, can be used now provided the linearity of the calorimeter response has not changed.

First we check that the CEM and CHA energy scales have not changed with respect to Run 0 and Run I. The energy of the calorimeter is set by the SCL scale factor, which is the ADC-to-GeV conversion factor. This is downloaded into the hardware so that the conversion is automatically done online for the L1 and L2 triggers. The same SCL is used for L3 and the offline. In addition, each tower has its own LER value, which is a relative scale factor that equalizes the tower response. The LERs are also downloaded to the hardware.

These constants may change with time because of calorimeter deterioration and new constants need to be periodically determined (changes are of a few %/year for the CEM). When the deterioration gets to a few %, new constants are downloaded into the hardware. In Run I tables of corrections between the downloading of new constants were available as a function of run number and used for the final analysis. For run II these corrections are done at the tower level when the offline reconstruction is made. So, to get all the constants correctly sometimes one has to rerun the calorimeter module for some of the recent runs. Beate Heinemann has implemented the code in the offline and keeps track of the corrections [9]. The changes in the online calibrations for the present data are shown in Appendix A.

After the CEM and the CHA scales are set, the jet energy scale is compared to Run I by comparing the results of γ-jet balance. For this study the photon is corrected with all the known corrections, while the jets are not corrected. This provides a comparison of raw jet energies in Run I and Run II (see Sec. 3.2).

3.1 CEM energy scale

The offline correction to the online ADC-to-GEV scale factor (SCL) of the CEM is set so that the reconstructed Z^0 mass is

$$m_{Z_0} = 91.05 \pm 0.29\ GeV$$

The online LERs are fine tuned with the offline LERs that are determined by equalizing the E/P value of every tower (see work of members of the ETF group [10]). The offline LERs are normalized so that the SCL value is unchanged. They are derived from data taken in the period Dec. 1, 2001 to May 2, 2002 (runs 133896-144220) and are applied offline. These LERs were incorporated into the online and downloaded into the hardware on June 19, 2002 (runs > 146507).

The CEM response is changing with time. This variation is determined by the time dependence of the average E/P as a function of run number [11]. A time-dependent correction has been implemented in offline V4.9.1 for runs # up to 152400. The online scale factor was changed for data after Run# 152400 (see Oct 2/2002 SCL change in Appendix A). The variation of CEM scale after run# 152400, though available, has not been included in the data used for the jet corrections. These corrections change the jet energy scale by $\sim 1\%$.

It is not clear that the same definition of CEM energy scale was used in QFL to define the absolute correction in Run I.

3.2 CHA and WHA energy scale

The CHA E scale is carried over from test beam data by radiative sources that check the tower response. One source got stuck during a run earlier in Run II so CHA source running has not been done since Nov. '91.

To monitor the time dependence of the calorimeter response we are using the minimum ionizing peak obtained with muons. The E-scale time dependence for the period February-June 2002 was studied by Michael Schmitt using high P_T muons [12], and by Robyn Madrak using J/ψ muons [13]. The results are shown in Fig.19. Variations of $< 1\%$ were observed during this period. The time dependence for the CHA E-scale has not been looked at again in time for this analysis and it is not included here.

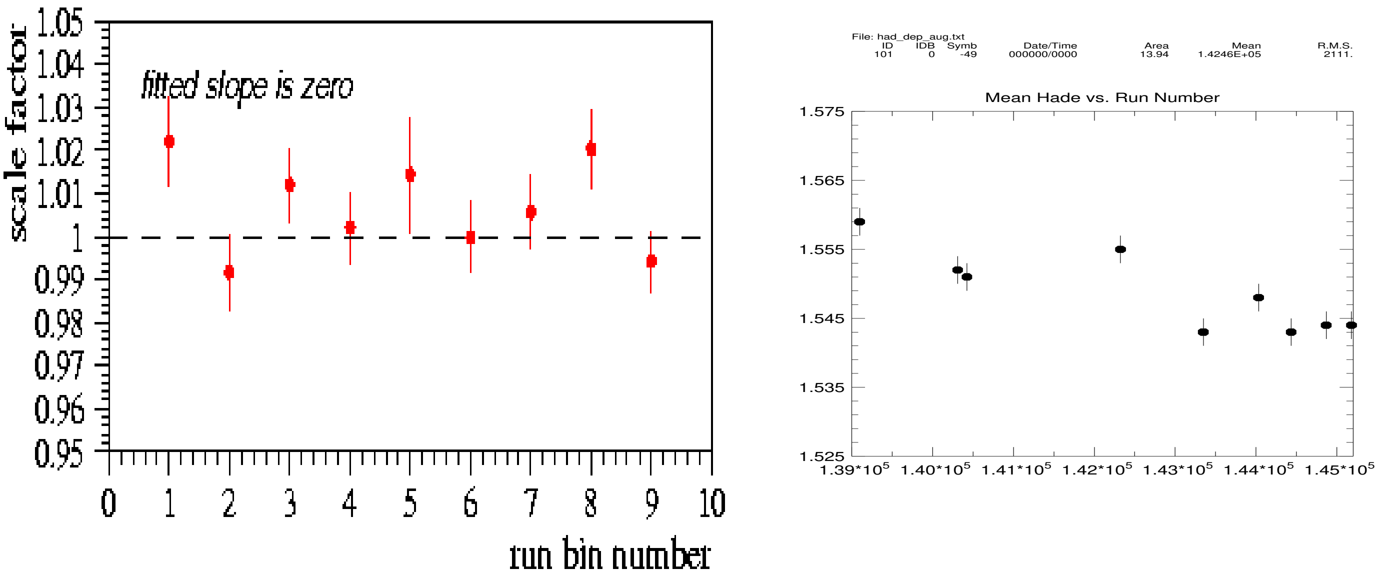

Figure 19: CHA: measurements of the muon MIP peak value as a function of time, using high P_T muons [12] (left) and J/ψ muons [13] (right).

In absence of source calibration runs, the CHA scale was set by comparing minimum-ionizing particle response in Run I and Run II data by Robyn Madrak who used J/ψ data [14], and by H.S. Kim [15], who used high P_T muons and later low P_T muons as well. Both measurements are shown in Fig.20. The ratio was found to be:

$$E_{Cal}^{MIP-RunII}/E_{Cal}^{MIP-RunI} = 0.960 \pm 0.005$$

This factor is included in offline V4.9.1 for data taken before run# 152400 (i.e.,

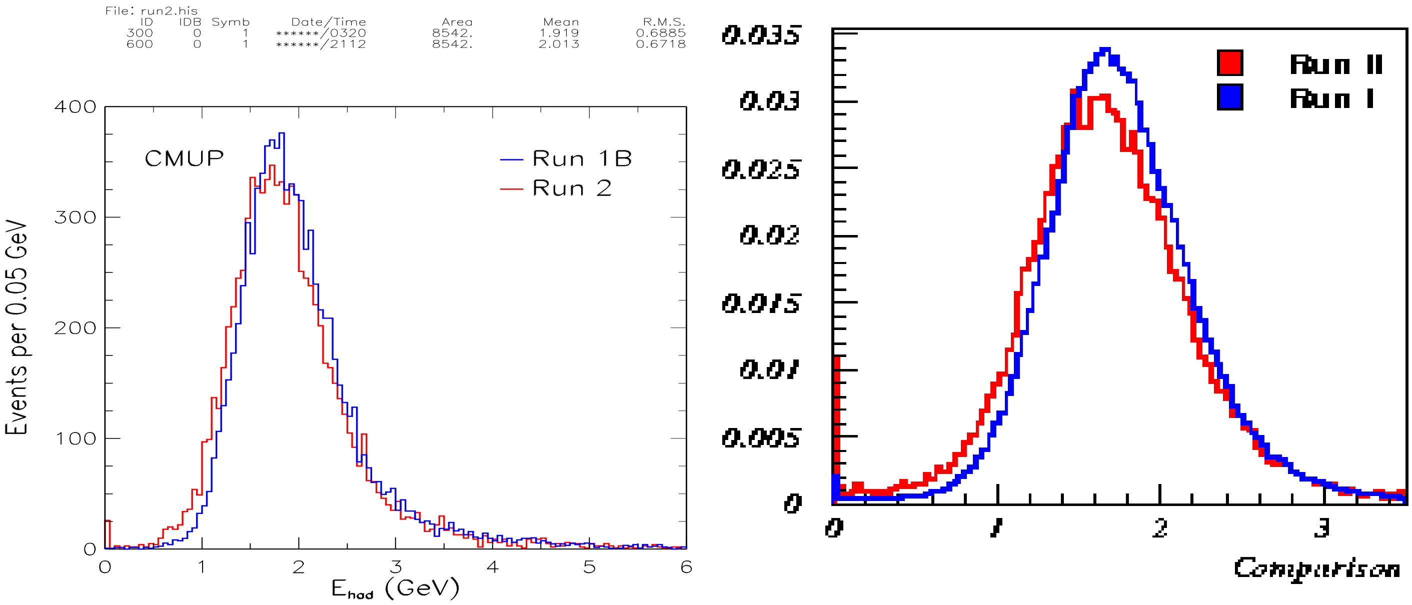

Figure 20: CHA measurements of MIP peak position in muons. Comparison of Run I and Run II, using high P_T muons [15] (left) and J/ψ muons [14] (right). The run II peak position is shifted to lower values by 4% in both data samples.

before Oct. 2, 2002) and in hardware for data taken after run# 152400 (see table in Appendix A).

For the WHA H.S. Kim [15] looked at CMX triggers for high P_T muons. This study shows about a 10% shift in the MIP position. See Fig. 21. Further studies made using J/ψ muons seems to be inconsistent with these data. [1]

3.3 Photon-Jet Studies

The CEM energy scale is set by electrons in the Z mass peak, the CHA energy scale is presently set by the MIP peak of low and high P_T muons. Jets include mostly low P_T pions and kaons in a region of non linearity of the calorimeters. As discussed in CDF-1513 [1] the Monte Carlo simulation is used to go from particles to jets. The simulation tuning in the central has used particles down to 0.5 GeV/c [5].

The raw jet energy scale in Run II can be checked using photon-jet balancing since the photon energy measured by the electromagnetic calorimeter is very precisely measured. In principle, after establishing the CEM and CHA energy scale as described above, photon-jet balancing results from Run II data should be identical to Run I. For this study, 29 pb^{-1} of photon-jet data from Feb 04, 2002 to August 10, 2002, processed with offline V4.5.3 (appropriately corrected offline) were used in

[1] In Feb. 03, this large shift in the WHA E-scale was confirmed by source data and downloaded into the hardware (see Appendix A).

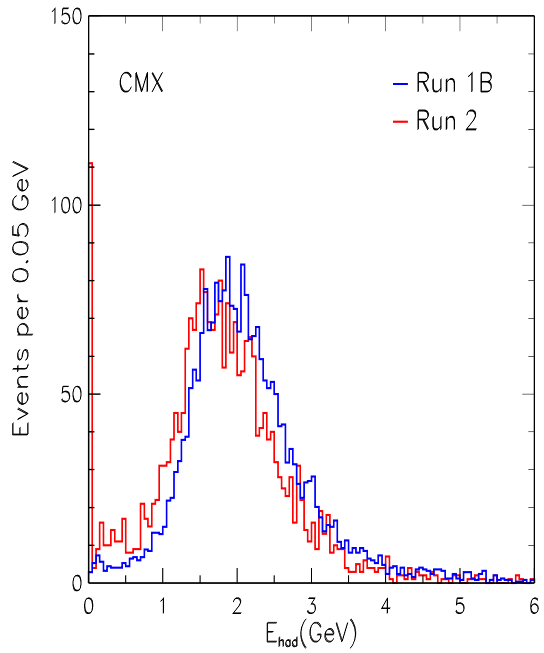

Figure 21: Comparison of the MIP peak position for WHA in Run 1B and II. Data are from the CMX triggers [15]. The Run II peak is shifted to lower values by $\sim$ 10%.

an analyses performed by G. Latino [16]. In Fig. 22 the quantity

$$f_b = \frac{P_T^{jet} - P_T^{\gamma}}{P_T^{\gamma}}$$

is plotted for the three different jet cone radii. The raw jet energy scale factor is then:

$$K_j = \frac{1+ < f_b^{runI} >}{1+ < f_b^{runII} >}$$

Table 4 shows the scale factors for the three different cone sizes.

Table 4: Scale factors for run II raw jet energies.

Cone Size	Raw Jets K_j
0.4	1.051$\pm$ 0.007
0.7	1.042$\pm$ 0.005
1.0	1.050$\pm$ 0.005

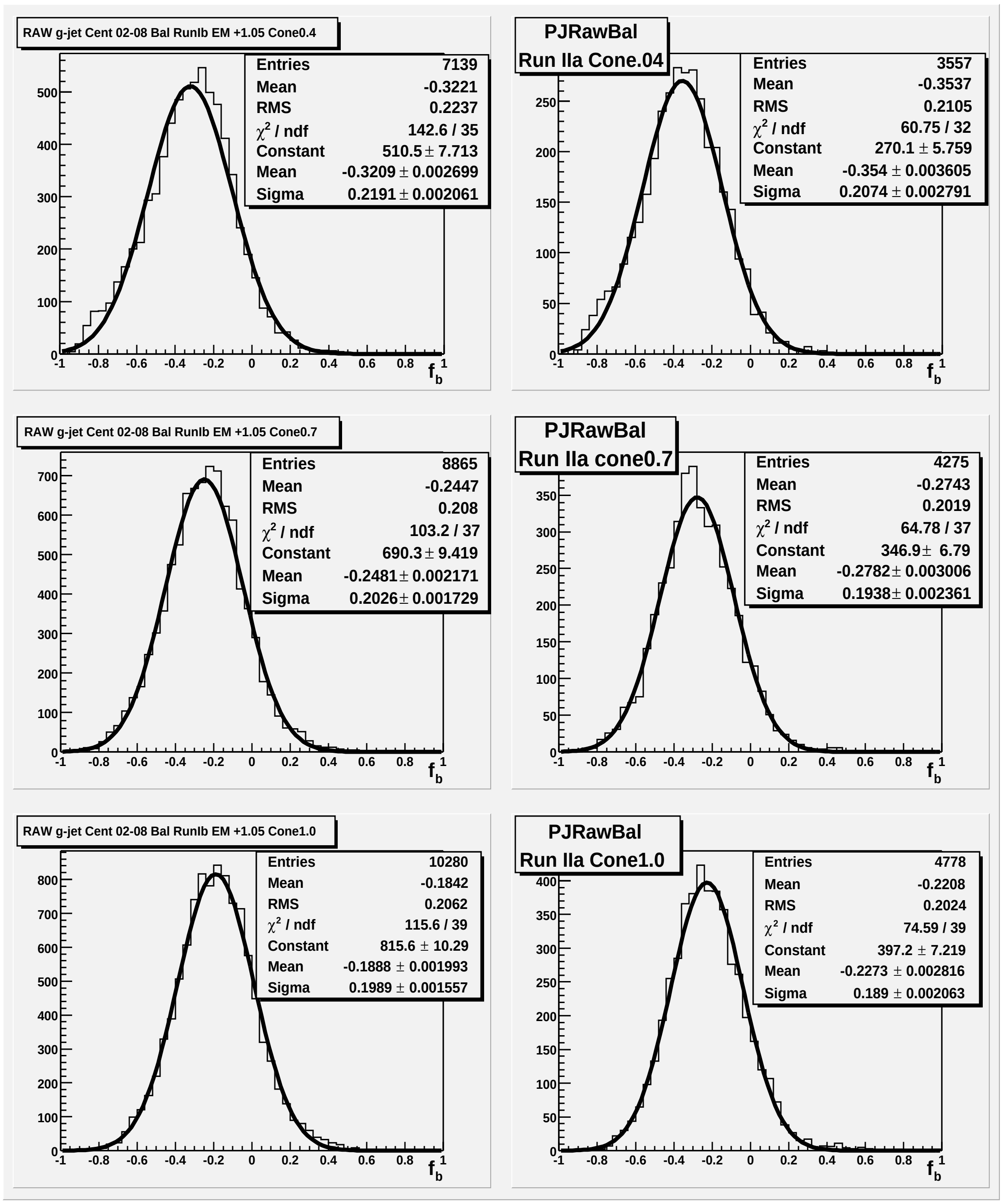

Figure 22: Fractional difference, f_b, between corrected photon and raw jet transverse momenta for Run Ib (left) and Run IIa (right) data for jet cone size R=0.4, 0.7, 1.0. These plots are used to tie the Run II raw jet energy to the Run I energy scale.

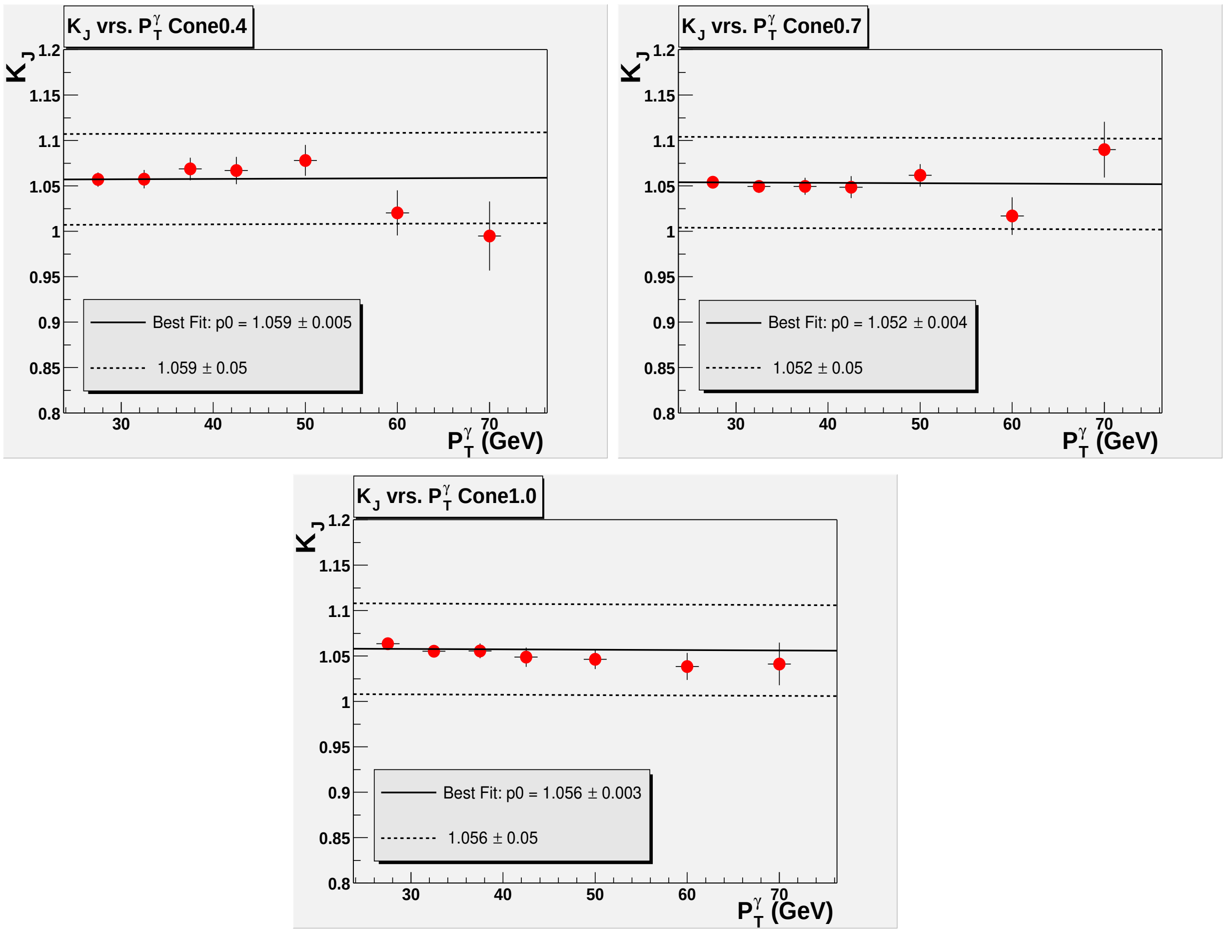

Figure 23: Ratio of raw jet E-scales for Run Ib and Run II data versus raw P_T of the jet, as obtained from γ-jet balance. Jet cone sizes are R=0.4 (top left), R=0.7 (top right), R=1.0 (bottom). The data sample used for these plots included 61 pb^-1 of integrated luminosity.

Updated results from an improved analysis performed with offline V4.9.1 on $\sim 61 pb^{-1}$ of data, taken from Feb. 04-2002 to Oct.-2003, were found to be consistent with those quoted in Table 4 [17].

Fig. 23 shows the K_j factors for the three cone sizes as a function of raw jet P_T as obtained with this larger sample. The jet energy is $\sim 5\%$ too low. The source of this discrepancy is not yet understood. Provided the scale of CEM and CHA are correct, either less energy is reaching the calorimeter or it is not being clustered in the same manner as in Run I. The clustering algorithm has been checked by many people and was found to be identical to Run I. A detailed Monte Carlo study is needed to understand the effect of any extra material in front of the calorimeter. A peculiar behavior of the f_b ratio at large EM fractions of the jets is still to be understood [16].

Another possible source of problems may arise from the fact that the signal integration time is now 132 ns rather then 396 ns as in Run I. Signal loss was found by running in Myron mode [18] and corrections were introduced in the SCL in December 2001 (see Appendix A). Additional studies were done by R. Erbacher to understand the behavior for low P_T particles in the jet [19]. The results indicate that further corrections are not needed. More work along these lines should be done. Also we need to investigate possible effects on jets as a function of E_T.

At this stage, we propose to correct the raw energy scale by the above factors and assign a 100% uncertainty. For example, for R=0.4 cone the correction factor is $(5.1 \pm 5.1)\%$.

4 Multiple Interaction Correction

At current luminosity and with 36 bunches, we expect on the average one interaction per beam crossing. However, since this has a Poisson distribution a fraction of the low cross section (Higgs, top, high E_T jets) events can have at least one overlapping minimum bias event. The energy from these minimum bias events may fall into the jet clustering cone and must be subtracted before the jet energy can be compared with theory predictions. A good indicator of the number of additional interactions in the same bunch crossing is the number of additional primary vertices in the event. The transverse energy in a random cone was measured in minimum bias data and parameterized as a function of number of vertices in the event [20]. See Fig.24. The slope of the line i.e. additional energy per vertex (overlapping minimum bias event) is given in Table 5. Efficiency and fake rate of the vertex reconstruction algorithm are different than in Run I and thus the multiple interaction energy per vertex is slightly different than in Run I. This correction is assigned an uncertainty of 100 MeV/vertex as in Run I.

Table 5: Additional energy per interaction in the jet cone from overlapping minimum bias events.

UDEVT (GeV)	Cone 0.4	Cone 0.7	Cone 1.0
Run II	0.260	0.781	1.581
Run I	0.297	0.910	1.858

5 Underlying Event Corrections

The energy from the spectator interaction that falls inside the jet clustering cone must be subtracted from the jet energy before it can be compared with theory calcu-

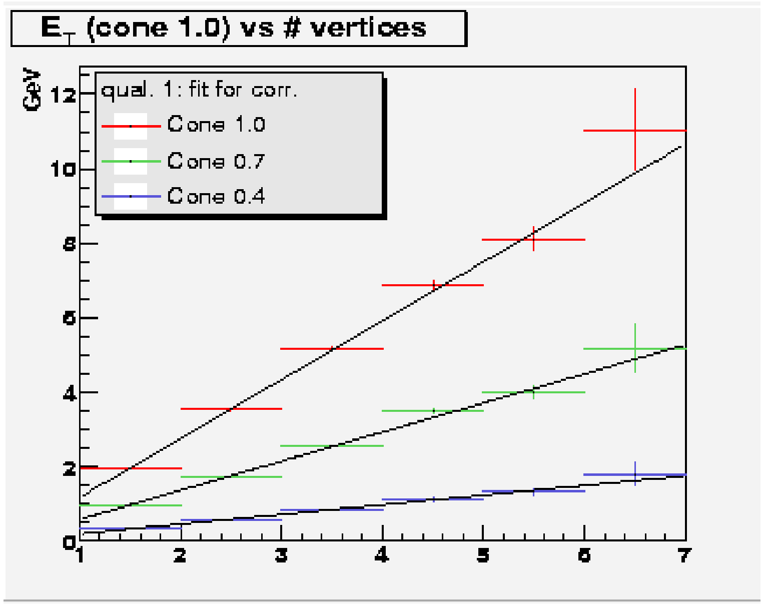

Figure 24: E$_T$ in cone of different radii as a function of the number of quality 12 vertices. The three straight lines correspond to R=0.4 (bottom), R=0.7 (middle), R=1.0 (top).

lations[2]. This correction may depend on the process under study. For, simplicity, we assume that the spectator interaction in any hard process are well modeled by minimum bias events. If required by the precision of the measurement, an additional process-dependent correction may be applied. The underlying event is measured from CLC-triggered events which have at least one quality 12 ($\geq$ 2 COT tracks) vertex as reconstructed by the Run II ZVertexColl vertex finder and given in Table 6 [20] along with the values obtained in Run I.

Table 6: Underlying Event Correction.

UD1EVT (GeV)	Cone 0.4	Cone 0.7	Cone 1.0
Run II	0.52	1.56	3.14
Run I	0.65	1.98	4.05

The Run II corrections are lower than in Run I. This can be explained by the different efficiency and fake rate of the vertex finders. In Run II, the efficiency to reconstruct vertices of quality 12 of events selected by the minimum bias trigger is 69.6%, while it was 47.7% in Run I for class 12 vertices. The larger inefficiency of the Run I finder will result in more events with two vertices to appear as one vertex

[2] Off course, one can model the underlying event and include it in the theory predictions.

event. These misrecontructed events will bias the correction values toward higher values. It was shown that one could retrieve the Run I values by using quality 60 vertices that have similar efficiencies that the Run I class 12 vertices [20].

In conclusion, the underlying event correction is lower in Run II, but because the vertex finding efficiency is higher than in Run I, the multiple interaction correction will be applied more often. Thus a better differentiation of the number of vertices is expected on an event-by-event basis. Note that this technique doesn't take into account the fact that the underlying event energy is expected to be different in the presence of jets. Therefore, one could obtain more accurate correction by looking at energy deposited in a cone of radius R at $\pm 90°$ to the leading jet in events containing a jet with $E_T = 5$ GeV. There are two such cones and one should use the cone with lower energy. This should remove small jets from gluon radiation, but in the absense of extra radiation it could bias the results to lower values.

6 Absolute Jet Energy Scale of the "Central" Calorimeter

The jet energy measured by the calorimeters must be corrected for any non-linearity and energy loss in the un-instrumented regions of each calorimeter. In addition, the energy deposited by a 50 GeV pion, which due to historical reason was used as the calibration point, may not be calibrated as 50 GeV and the data must be corrected.

The conversion factor from calorimeter energy to particle-level energy is called absolute energy correction. This correction depends on the jet fragmentation properties, hence depends on the non-linearity of the calorimeter and the difference in calorimeter response to π^0 and $\pi^{\pm}$. The correction also depends on the cone size used for the jets.

In Run I the absolute corrections were determined in 1991 using jets generated with a tuned MC [1]. The same corrections can be used in Run II as long as non-linearity and relative response to π^0 and $\pi^{\pm}$ have not changed since 1991, except for a scale factor. We expect, however, to do better in Run II because the new simulation allows for tuning of the lateral shower shape (in progress). We use isolated tracks from minbias events [6] and high P_T isolated tracks trigger data [21] for the tuning.

The corrections, determined with QFL V3.20, were parameterized as piece-wise quadratic functions with a break point at $P_T = 100$ GeV (see Table below).

$$f_{abs} = (P_0 + P_1 \cdot P_T + P_2 \cdot {P_T}^2)/100$$

The absolute corrections are shown in Fig. 25. These are the functions that are used in Run II at this time.

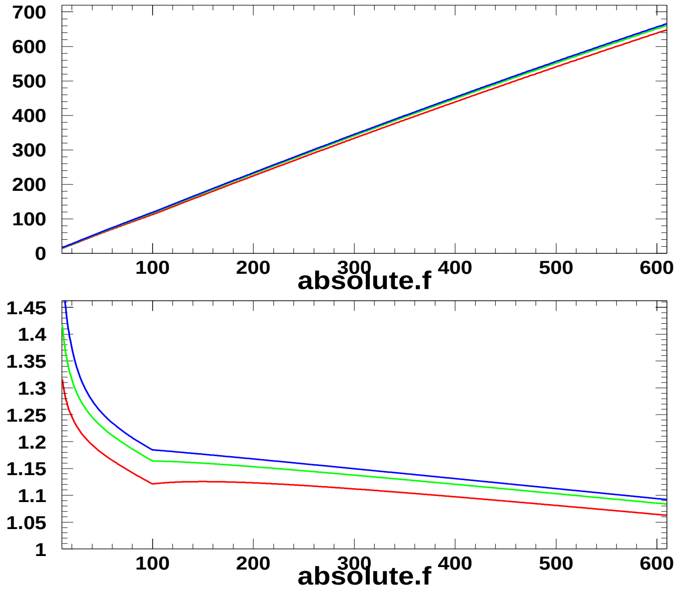

Figure 25: Corrected energy as function of raw energy (top) and ratio of corrected and raw energies (bottom). The three curves are for R=0.4 (lower), R=0.7 (middle), R=1.0 (higher).

Table 7: Parameters used in Run I for the absolute jet energy scale corrections for cone sizes R=0.4, 0.7 and 1.0.

	$P_T \leq 100.0$			$P_T > 100.0$		
	0.4	0.7	1.0	0.4	0.7	1.0
P_0	1.37	2.09	3.29	-4.03	-1.49	-0.37
P_1	1.1946	1.227	1.2229	1.1794	1.197	1.20704
P_2	-0.0008724	-0.000839	-.0007133	-0.0001805	-0.000182	-.0001878

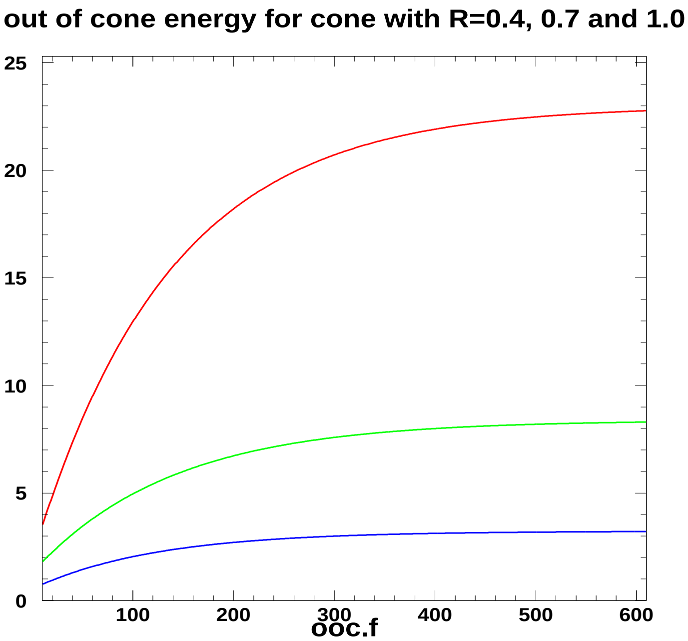

Figure 26: Out-of-cone energy as a function of P_T for three cone sizes. The curves are for R=0.4 (top), R=0.7 (middle), R=1.0 (bottom).

7 Out-of-Cone Corrections

The jet clustering may not include all the energy from the initiating parton. Some of the partons generated during fragmentation may fall outside the cone chosen for clustering algorithm. Out-of-cone corrections were applied in order to correct the particle-level jet energy to the parton energy (as much as it is theoretically allowed). These corrections are completely independent of detector/calorimeter performance and depend on the parton fragmentation functions. The corrections derived for Run I are being used for Run II data. The additional energy is parameterized as

$$P_T(OC) = A[conesize] * (1.0 - B[conesize] * e^{-C[conesize]*pt)};$$

and shown in Fig. 26. The parameters for the three cones sizes are given in Table 8.

8 Systematic Uncertainties

Details of the systematic uncertainties on the current jet corrections can be found in CDF-6419 [8]. We note here the following contributions to the systematic uncertainties.

- The raw energy scale outside $0.2| \leq \eta| \leq 0.6$ region has $\sim 2\%$ uncertainty relative to the scale in the central region, as discussed in Sec. 2.4.

Table 8: Out-of-cone energy parameters (taken from Run I code).

	A	B	C
0.4	22.999	0.915	0.00740
0.7	8.382	0.846	0.00728
1.0	3.227	0.832	0.00817

- The raw jet energy scale of the central CDFII calorimeter has $\pm 5\%$ uncertainty (from photon-jet balancing).
- The underlying event energy has an uncertainty of $\pm 30\%$ (historically it was obtained by comparing UE in dijet and minimum bias events).
- Uncertainty in "absolute energy scale" arises from uncertainty in charged pion response measurement in test-beam and $p\bar{p}$ data and jet fragmentation functions. It was around 2.5% in Run I [22]. An additional systematic uncertainty needs to be assigned in run II. See discussion in Ref. [8].
- Uncertainties in the out of cone and multiple interaction corrections can be taken to be the same as in Run I [2].

9 Summary and Conclusions

Preliminary jet corrections for Run II data are available for general use but we need to do much more detailed work to understand certain features and improve the precision. Separate relative corrections are provided for data and Monte Carlo because of discrepancies between the η dependence of data and simulation.

Major problems seem to be:

- Understand the 5% disagreement between Run I and Run II raw jet energy scale as determined from γ-jet balance.
- Understand the large disagreement between data and MC at $|\eta| \sim 1$ (WHA region).
- Do the tuning of the lateral shower shape in the simulation.
- Understand the big disagreement between data and MC for $|\eta| > 2$.
- Use time dependent tower corrections for the plug calorimeters in order to correct for time dependent gains.
- Redo the absolute and out-of-cone corrections for CDFII.

A Appendix A: Changes in the online calibration constants of the calorimeters

Dates when the SCLs and LERs were downloaded to the hardware are shown in the Table below. The offline corrections for the in between periods were implemented by Beate Heinemann [9].

Date	Detector	Change	Comment
Dec 07/01	All	many	starting point for SCL and LERs
Apr 19/02	WHA LER		Nicolay updates, no SCL change
Jun 19/02	CEM LER		from Eva and Larry
Sep 11/02	PEM, PHA LER		4 outer eta rings towers, PMT HV change
Oct 02/02	CEM SCL	+3%	Larry's E/P drift
Oct 02/02	CHA SCL	+4%	Muons E-scale change (Hyunsoo)
Feb 06/03	CEM LER		Larry's update
Feb 06/03	PEM LER,SCL		based on source runs
Feb 06/03	PHA LER,SCL		based on source runs
Feb 26/03	WHA LER	+(8-10)%	no SCL change (Nov/01-Feb/03 source data)
May 28/03	PEM, PHA LER	+3%	The 3% is only for the high η towers

In Dec. 2001 the SCL were increased due to new calibrations as well as to take into account for loss of signal outside the 132 ns ADC gate. Changes due to signal loss are: CEM (+2%), CHA(+6.5%), WHA(+6.5%), PEM(+2%), PHA(+2.7%).

The jet corrections for Winter Conferences use data up to Jan 12/03, so changes after this date are not important for this work. They are shown here for completeness. An additional correction that is made on the offline only [9] is due to cross calibrations of the plug sources [4], which were established in mid-March, so have not been applied for the winter corrections These corrections are shown in Table 9.

Table 9: Plug sources corrections by quadrant

side	Q1	Q2	Q3	Q4
East	1.000	1.0058	1.0131	1.0372
West	1.0568	1.0218	1.0478	1.0319

For instruction on how to use the corrections see the documentation on the jet correction WEB page at:

http://www-cdf.fnal.gov/internal/physics/top/jets/corrections.html

References

[1] L. Keeble, B. Flaugher, *New jet correction function QDJSCO 2.0*, CDF-1513 (July 1991).

[2] L. Galtieri, J. Lys, *How well do we understand jets in Run I? Study of the Jet E-scale for raw jet $E_T > 8$ GeV*, CDF-3983 (March 1997).

[3] W. Sakumoto et al., ETF meetings.

[4] H.S. Budd, W.K. Sakumoto, *Determining Gains of Plug Towers using Plug Laser and Source Data*, CDF-6433 (April 2003)

[5] C. Currat, Soon Yung Jun, R. Eusebi, A. Hocker, P. Savard, *Single pion response in the CDF calorimeters and tuning of GFLASH*, CDF-5886 (March 2002).

[6] S. Demers et al., *Response of the Central Calorimeter to low momentum, isolated hadrons in Run2*, CDF-5874 (March 2002).

[7] C. Currat, L. Galtieri, J. Lys, *Comparison of uncorrected jet P_T in data and Monte Carlo after time dependent corrections in the plug calorimeters*, CDF-6420 (June 2003).

[8] J-F. Arguin et al. (Jet correction group), *Systematic Uncertainties associated with Jet corrections for Winter 2003 Conferences*, CDF-6419 (June 2003).

[9] B. Heinemann, *Offline Calibration of the Calorimeter*, CDF-6406 (April, 2003)

[10] M. Coca et al., *A first look at Run 2 High P_T Electrons*, CDF-5803 (February 2003).

[11] L. Nodulman, *A MIN-Bias Calorimeter Ntuple*, CDF-6364, (April 2003). It includes a plot obtained from the electron Ntuple (L. Nodulamn, CDF-5909).

[12] Michael Schmitt, talk at the Jet Correction meeting of August 7, 2002.

[13] Robyn Madrak, talk at the Jet Correction meeting of August 7, 2002.

[14] Robyn Madrak, talk at the Jet Correction meeting of May 29, 2002.

[15] H.S. Kim, *MIP Energy Scale Comparisons of CHA/WHA between Run I and Run II*, CDF-6392, in preparation. The E-scale checks were shown in talks at the Jet Correction meetings of Sept. 4, 2002 (high P_T muons) and of 11/13 and 12/11, 2002 (low P_T muons).

[16] G. Latino, *Jet EM Fraction Studies: RunI-RunII Comparison on Gamma-Jet Data*, CDF-6152 (March 2003). Results used for the jet corrections were done on an earlier set of data.

[17] G. Latino, talk at the Jet Correction meeting of March 5, 2003.

[18] R. Erbacher, *Calorimeter ADC Gate Timing*, CDF-5797 (Dec. 2001).

[19] R. Erbacher, *Effect of the Run II Electronics on the Jet Energy Scale*, CDF-6235, in preparation. See talk at the Jet Correction meeting of Nov. 13, 2002.

[20] J.-F. Arguin, B. Heinemann, *Underlying Event Corrections in Run II*, CDF-6239 (February 2003).

[21] M. Baumgart, M. Shochet, *Calorimeter response to Isolated High P_T Tracks*, CDF-6093 (August 2002).

[22] S. Behrends,*A plot of the systematic uncertainty on jet P_T*, CDF-3550 (February 1996).